THE JOURNAL OF PHYSICAL CHEMISTRY C

Article

pubs.acs.org/JPCC

Dehydrogenation Mechanism of Monoammoniated Lithium Amidoborane [$Li(NH_3)NH_2BH_3$]

S. Bhattacharya,[†,#] Zhitao Xiong,[‡] Guotao Wu,[‡] Ping Chen,[‡] Y. P. Feng,[§] C. Majumder,[∥] and G. P. Das*[,†]

[†]Department of Materials Science, Indian Association for the Cultivation of Science, Kolkata 700 032, India

[‡]Dalian Institute of Chemical Physics, Dalian, China

[§]Department of Physics, National University of Singapore, Singapore

[∥]Chemistry Division, Bhabha Atomic Research Centre, Mumbai 400 085, India

Supporting Information

ABSTRACT: Monoammoniated lithium amidoborane has been experimentally synthesized. When this is heated to a temperature of 40−55 °C, this releases 9−11 wt % hydrogen. First-principles density functional calculations have been carried out to understand the underlying mechanism of dehydrogenation. Theoretical results predict that the reaction is a three-step process; each step consists of 3.7, 3.9, and 4.0 wt % H_2 uptake with an altogether capacity of 12 wt % dehydrogenation. Whereas the first dehydrogenation is a direct interaction between lithium amidoborane and NH_3 monomers, the subsequent reaction steps lead to further dehydrogenation, provided that the activation barrier falls within reasonable limits, and this has been achieved by forming higher-order nanoclusters of $[Li(NH_2)\text{-}NH_2BH_3]_n$.

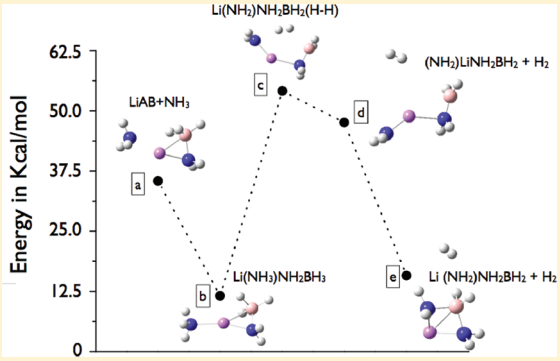

1. INTRODUCTION

Among the light metal complex hydrides, ammonia borane (NH_3BH_3) [AB] is considered to be one of the most promising hydrogen storage materials because of its high hydrogen content (19.6 wt %) capacity.[1] The pristine AB molecule contains both hydridic B−H and protic N−H bonds and a strong B−N bond so that hydrogen release from solid AB is more favorable than dissociation to ammonia and diborane under most conditions.[1] However, subsequent release of hydrogen with the increase of temperature leads to the generation of volatile toxic species, such as borazine,[2] which can poison the fuel cells. This results in a poor H-release kinetics and dehydrogenation mechanism from pristine AB, which needs further improvement for its effective practical implementations in on-board H-storage devices. One way to improve the performance of AB is substituting one H atom in the [NH_3] unit by metals, such as Li, Na, etc., to form lithium amidoborane ($LiNH_2BH_3$)[LiAB] and sodium amidoborane ($NaNH_2BH_3$)[NaAB] with a gravimetric efficiency of 10.9 and 7.5 wt %, respectively.[3] These materials have also been highlighted as some of the best potential hydrogen-storage materials in the 2008 DOE hydrogen program annual progress report.[4] With more electrons being donated from metal to $[NH_2BH_3]^-$ ions, the hydridic B−H bond of $[NH_2BH_3]^-$ ions is elongated, which enhances its activity as compared with those in pure AB. Therefore, the reaction barrier between $[NH_2BH_3]^-$ ions would be lower than that between two neutral NH_3BH_3 molecules. In addition, the charged $[NH_2BH_3]^-$ ion creates more polar surroundings compared with the symmetric NH_3BH_3 complex. The obvious consequence of this is a much faster reaction kinetics in metal−amidoboranes, compared with the same for pristine AB.[5] It has been reported that a lower dehydrogenation temperature (≈90 °C) can be achieved in LiAB compared with pristine AB (≈110 °C).[3]

To improve the operating properties of these materials, such as rapid H_2 release near room temperature, it is vital to understand the underlying mechanism for the release of H_2. What is known is that the $[NH_2BH_3]^-$ unit attracts the metal cation Li^+, thereby enhancing the reactivity of the hydridic B−H bond. This results in a BH−NH interaction between the adjacent units of LiAB. The obvious consequence of this is the reduction of the lowered dehydrogenation temperature.[5] Recently, Xia et al. have experimentally synthesized monoammoniated LiAB [$Li(NH_3)NH_2BH_3$], which shows more favorable dehydrogenation characteristics in the temperature range of 40−70 °C.[6] However, there is still no acknowledged model calculation to explain the detail decomposition mechanism following this experimental finding. To theoretically model this reaction mechanism, one has to find reaction pathways, where the activation barrier lies in the range of 20−25 kcal/mol, which is acceptable for gas-phase calculations.

Received: June 15, 2011
Revised: March 15, 2012
Published: March 16, 2012

   dx.doi.org/10.1021/jp210315u | J. Phys. Chem. C 2012, 116, 8859−8864

Here, we explore an alternative route to synthesize monoammoniated LiAB and report our first-principles density functional investigation to realize the reaction mechanism of hydrogen release from monoammoniated LiAB [$Li(NH_3)$-NH_2BH_3]. Our theoretical results predict that the reaction is a three-step process; each step consists of 3.7, 3.9, and 4.0 wt % H_2 release with an altogether capacity of ≈12 wt % dehydrogenation. However, experimentally, we could get ≈11 wt % H_2 release at a temperature of 55 °C. According to our findings, the first dehydrogenation is a direct interaction between LiAB and NH_3 monomers. The subsequent reaction steps lead to further dehydrogenation, provided the activation barrier falls within the above-mentioned realistic limits. We have shown how this can be achieved by forming higher-order nanoclusters[7] of $[Li(NH_2)NH_2BH_2]_n$.

2. COMPUTATIONAL DETAILS

We performed density functional calculations using Gaussian 03 software[8] with the B3LYP functional[9−12] and the 6-311++G(d,p) basis set. The 6-311++g(d,p) basis set includes diffuse functions. All the ground-state geometries were optimized with B3LYP (Beckes hybrid exchange functional and the correlation functional of Lee, Yang, and Parr) in Gaussian 03. After geometry optimizations, the energy values are calculated with second-order perturbation theory [MP2].[13]

In a recent article,[14] it has been found that B3LYP does not describe dative bonds well, sometimes giving qualitatively wrong trends. Therefore, a more rigorous approach needs to be implemented by either the G3 or the G4 composite technique. In view of this, to cross-check our calculation error bar for a system like LiAB, we have estimated the B−H and N−H bond energies using the G3 level of accuracy and compared this with the calculated B−H/N−H bond energies using the B3LYP/MP2 level of accuracy. While the B−H bond energy of LiAB is found to be 43.49 kcal/mol (using G3) and 37.57 kcal/mol (using B3LYP/MP2), respectively, the N−H bond energy is found to be 49.15 kcal/mol (using G3) and 42.12 kcal/mol (using B3LYP/MP2), respectively. Since values compare reasonably well, the single-point energy of MP2 is expected to be of a similar quality as of G3/G4, at least for this particular system. Moreover, we have also examined the final optimized structure of monoammoniated LiAB [LiAB + NH_3] using these two types of approaches [e.g., G3 vs B3LYP], as provided in the Supporting Information. Since the difference of bond length is in the third decimal place, we are inclined to believe that the error bar in our calculated numbers does not affect the conclusions arrived at in this paper.

Finally, we have performed vibrational analysis to examine the stability of the clusters. All the stable clusters reported in this paper have real frequencies. From frequency analysis, the transition states (TS) are detected. Transition states are then connected with stable reactants and products via intrinsic reaction coordinate (IRC)[15] calculations. This helps us to trace the reaction path from the TS to reactant(s) and product(s), which is essential for understanding the reaction mechanism. The IRC is thus a simple, yet effective, approach for probing complicated reaction processes. However, for a more rigorous methodology, first-principles molecular dynamics along the intrinsic reaction path needs to be performed.

3. RESULTS AND DISCUSSION

3.1. Experimental Section. In this section, we presented an alternative route to the synthesis of monoammoniated lithium amidoborane. Chemical reaction between $LiNH_2$ and NH_3BH_3 in THF was employed to produce $LiNH_2BH_3$ and NH_3, and then, NH_3 adducts to $LiNH_2BH_3$ during the process of evaporating THF at ambient temperature (<25 °C) to form the complex hydride $Li(NH_3)NH_2BH_3$. This is a similar kind of reaction as the synthesis of $Ca(NH_3)_2(NH_2BH_3)_2$ using the chemical reaction between $Ca(NH_2)_2$ and NH_3BH_3. $LiNH_2$ and NH_3BH_3 were Sigma Aldrich products with claimed purities of 95% and 97% and used as received. Reaction between $LiNH_2$ and NH_3BH_3 in THF solution was conducted within a stirred high-pressure autoclave. Typically, 0.008 mol or 184 mg of $LiNH_2$ powder was put into the NH_3BH_3−THF solution (0.008 mol of NH_3BH_3 in 30 mL of THF), and the suspension was stirred vigorously at ambient temperature. To release hydrogen from the resulting $Li(NH_3)NH_2BH_3$, the autoclave was rapidly heated to the given temperature, and meanwhile, the inside pressure was recorded using a digital gauge. At the completion of desorption, gas in the autoclave was analyzed by a mass spectrometer, and every time, hydrogen was the only detectable gas. Therefore, using the ideal gas equation, the amount of evolved hydrogen can be determined. As shown in Figure 1, 9−11 wt % hydrogen was evolved from $Li(NH_3)NH_2BH_3$ at temperatures of 40−55 °C.

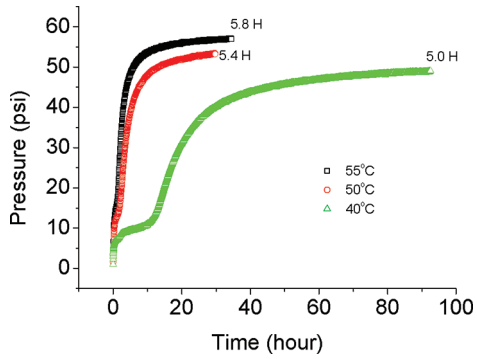

Figure 1. Hydrogen release pressure as a function of time at different temperatures.

3.2. Monoammoniated LiAB [$Li(NH_3)NH_2BH_3$] Monomer. On exposure of a single LiAB molecule to ammonia in a 1:1 ratio (Figure 2, step a), it results in adsorption of NH_3 in LiAB by forming a complex structure called monoammoniated

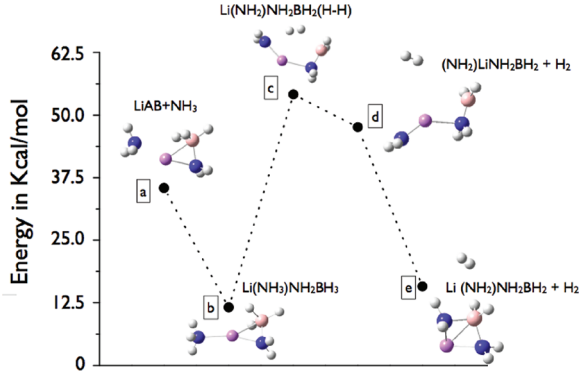

Figure 2. Reaction path of LiAB and NH_3 monomers.

dx.doi.org/10.1021/jp210315u | J. Phys. Chem. C 2012, 116, 8859−8864

LiAB [$Li(NH_3)NH_2BH_3$] with NH_3 getting attached to the Li site of LiAB (Figure 2, step b). NH_3 is bound with LiAB by a weak chemical bond in a similar way to that in the well-known lithium-based ammonia coordination compounds, such as ammonia lithium chloride[16] and ammonia lithium borohydride,[17] in which the NH_3 is bound to Li^+ through a coordination bond. We now explore the possibility of dehydrogenation of this newly formed coordination compound, viz. monoammoniated LiAB [$Li(NH_3)NH_2BH_3$] in different steps.

Dehydrogenation of $Li(NH_3)NH_2BH_3$ Monomer. To gain insight into the H_2-release mechanisms in $Li(NH_3)NH_2BH_3$, we first studied the different possible pathways of dehydrogenation from $Li(NH_3)NH_2BH_3$ monomer in the gas phase, together with their relative activation barriers. After carrying out a very systematic and thorough search, we report here a specific reaction pathway (Figure 2), which has the minimum activation barrier. To our best belief, no other intermediate structure (transition state) is possible where the reaction is more favorable. We have found a transition state (Figure 2, step c) where the hydridic B−H bond in the [NH_2BH_3] unit interacts with the protic N−H bond of NH_3, which, in turn, leads to hydrogen release from the system as a first dehydrogenation process (Figure 2, step d). Our calculation yields that the lowest activation barrier required for such a transition state is 18.4 kcal/mol (Figure 2). The corresponding imaginary frequency is 280.93 cm^{-1}. This result is quite reasonable as it suggests that the dehydrogenation process can occur at an ambient temperature, as also found experimentally.[6] Comparable activation barriers of LiAB in different dehydrogenation routes have already been estimated by several other groups.[18,19] In a pristine LiAB cluster $[LiNH_2BH_3]_2$, a similar activation barrier has been estimated by D. Y. Kim et al., which is found to be 33 kcal/mol.[20] This signifies a clear indication that the coordination bonds formed between NH_3 and Li^+ are beneficial to enhancing the interaction between the hydridic B−H bonds and protic N−H bonds, resulting in hydrogen release at lower temperature. When the first dehydrogenation is finished, we notice formation of a metastable product, $(NH_2)LiNH_2BH_2$ (Figure 2, step d), which, on optimization, relaxes its ionic positions and forms a stable complex, $Li(NH_2)NH_2BH_2$ (Figure 2, step e). The relaxation energy is found to be 23 kcal/mol. Thus, the overall reaction proceeds as follows

$$Li(NH_3)NH_2BH_3 \rightarrow (NH_2)LiNH_2BH_2[H{-}H] \rightarrow (NH_2)LiNH_2BH_2 + H_2 \quad (1)$$

$$(NH_2)LiNH_2BH_2 \rightarrow Li(NH_2)NH_2BH_2 + \Delta H \quad (2)$$

After the first hydrogen release, the second dehydrogenation takes place from this optimized complex $Li(NH_2)NH_2BH_2$. Accordingly, for the second dehydrogenation, we start finding suitable pathways for appropriate transition states so that the activation barrier falls in suitable limits. Among many different pathways, the lowest activation barrier is estimated as 25.14 kcal/mol (Figure 3).

The reaction looks like

$$Li(NH_2)NH_2BH_2 \rightarrow Li(NH)NH_2BH(H{-}H) \rightarrow Li(NH)NH_2BH + H_2 \quad (3)$$

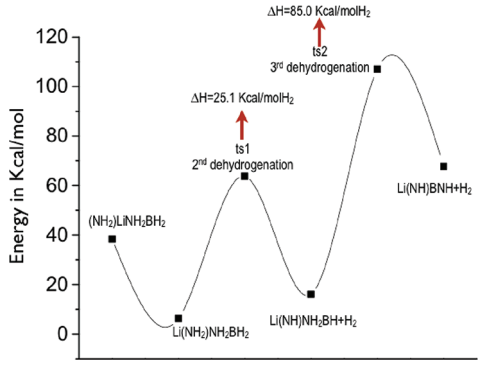

Figure 3. Reaction path of LiAB and NH_3 monomers.

Thereafter, the third dehydrogenation takes place from $Li(NH)NH_2BH$, followed by a transition state with an activation barrier estimated to be ≈85 kcal/mol (Figure 3). The reaction looks like

$$Li(NH_2)NH_2BH_2 \rightarrow Li(N)NH_2B(H{-}H) \rightarrow Li(NH)BNH + H_2 \quad (4)$$

From our experiment, we have found hydrogen release at 40−55 °C. Earlier, Xia et al.[6] also reported that the dehydrogenations take place at a temperature range between 40 and 70 °C. From our theoretical calculations, the activation barrier for the first dehydrogenation falls within a reasonable limit; however, the second and third dehydrogenations are consistently higher. Therefore, the formation of the monoammoniated LiAB complex [$Li(NH_3)NH_2BH_3$] is a direct interaction between LiAB and NH_3 monomers, and the immediate next consequence is a spontaneous hydrogen release named as first dehydrogenation. The subsequent reaction steps lead to further dehydrogenation, provided that the activation barrier falls within reasonable limits, and this can be achieved by forming higher-order nanoclusters[7] of $[Li(NH_2)NH_2BH_3]_n$, as described below.

3.3. $[Li(NH_2)NH_2BH_3]_n$ Cluster. From eq 2, we see that, after the first dehydrogenation, a metastable product (NH_2)-$LiNH_2BH_2$ is formed, which, after ionic relaxation, released 23 kcal/mol of energy, and this metastable product is converted into a stable monomer of $Li(NH_2)NH_2BH_2$. Instead of this, we explore the possibility of formation of a stable cluster of $[Li(NH_2)NH_2BH_2]_n$. Therefore, in this model calculation, n units of metastable [$(NH_2)LiNH_2BH_2$], after ionic relaxation, release energy and thereby get optimized as a stable cluster of $[Li(NH_2)NH_2BH_2]_n$. With suitable values of n varying from n = 2 to n = 6 (Figure 4), we have estimated the corresponding cluster stability (S) (see Figure 4) defined as

$$S = \{E_{total}[Li(NH_2)NH_2BH_2]_n - n \times E_{total}[(NH_2)LiNH_2BH_2]\}/n \quad (5)$$

We can see from Figure 4 that, when the cluster size goes up, the relative cluster stability becomes more negative and converges around $n \geq 6$. However, we found that doing an accurate quantum chemical model calculation for finding different transition states (TS) with a sufficiently large basis [e.g., 6-311++G(d,p)] is computationally extremely costly for an n = 6 cluster. It should be noted from Figure 4 that the relative stability for a cluster with n = 3 and n = 6 are

dx.doi.org/10.1021/jp210315u | J. Phys. Chem. C 2012, 116, 8859−8864

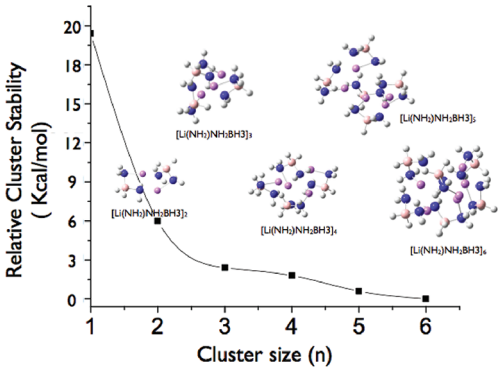

Figure 4. Stability vs cluster size (n) plot for different $Li(NH_2)$-$NH_2BH_3]_n$ clusters.

comparable and the difference is in the third decimal place of magnitude. Thus, the dehydrogenation behavior from both the clusters should be nearly comparable. Therefore, up to the second dehydrogenation, we extended our calculation with a cluster size varying from $n = 2$ to $n = 6$, but for the third and final dehydrogenations, we restrict ourselves to a cluster size of $n = 3$. This is because we wanted to see the trends in activation barrier (for different TS) on dehydrogenation when (NH_2)-$LiNH_2BH_2$ forms a stable nanocluster as compared to its monomer results, as discussed earlier. However, it should be remembered that, when we take a cluster of size n, for both second and third dehydrogenations, the total $2nH_2$ is expected to be released with nH_2 in each step. Thus, for a cluster of size $n = 3$, a total of six H_2 molecules will be released.

Dehydrogenation Reaction of $[Li(NH_2)NH_2BH_2]_3$ Cluster. The reaction profile for the second dehydrogenation process of the $[Li(NH_2)NH_2BH_2]_3$ system is shown in Figure 5. Three

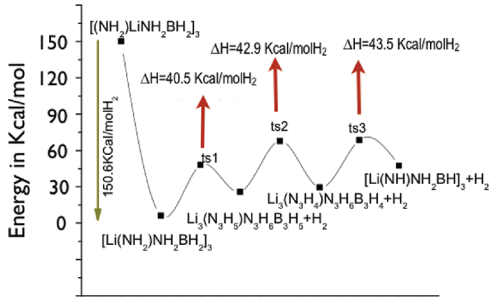

Figure 5. Second dehydrogenation from the $[Li(NH_2)NH_2BH_2]_3$ cluster.

units of metastable $[(NH_2)LiNH_2BH_2]$ on ionic relaxation forms a stable complex $[Li(NH_2)NH_2BH_2]_3$, and the corresponding relaxation energy is estimated to be 150.6 kcal. From this $[Li(NH2)NH_2BH_2]_3$ cluster, we search for three consecutive hydrogen releases via a suitable TS with the lowest possible activation barriers.

The estimated activation barrier for three consecutive H_2 releases are, respectively, 40.5, 42.9, and 43.5 kcal/mol. At first glance, these three reaction barrier values appear to be high. However, if we consider the relaxation energy (150.6 kcal) released (see Figure 5) during formation of such a cluster, this energy is sufficient to help the system to overcome three such consecutive reaction barriers.

It is to be noted that, for the second dehydrogenation, the energy barriers for successive releases of H_2 are superimposed on a more-or-less linear increase of energy for the corresponding intermediate products. It might appear that, for larger clusters, this trend in slope might lead to the final product energy (or its precursor ts3) being larger than the formation energy itself of the cluster. From our test calculations, we have ensured that, for a higher-order cluster, this linear increase will taper off. Thus, according to this model calculation by considering the $[Li(NH_2)NH_2BH_2]_n$ cluster, the second dehydrogenation is clearly a barrier-less spontaneous phenomenon, which is in good agreement with our experimental observation. Therefore, the overall reaction mechanism for the second dehydrogenation is given below for cluster size $n = 3$

$$[Li(NH_2)NH_2BH_2]_3 \rightarrow Li_3(N_3H_5)N_3H_6B_3H_5(H{-}H) \rightarrow Li_3(N_3H_5)N_3H_6B_3H_5 + H_2 \quad (6)$$

$$Li_3(N_3H_5)N_3H_6B_3H_5 \rightarrow Li_3(N_3H_4)N_3H_6B_3H_4(H{-}H) \rightarrow Li_3(N_3H_4)N_3H_6B_3H_4 + H_2 \quad (7)$$

$$Li_3(N_3H_4)N_3H_6B_3H_4 \rightarrow Li_3(N_3H_3)N_3H_6B_3H_3(H{-}H) \rightarrow Li_3(N_3H_3)N_3H_6B_3H_3 + H_2 \quad (8)$$

Next, we proceed to find the third and final dehydrogenations from the $[Li(NH)NH_2BH]_3$ cluster. In a similar fashion as discussed above, we have estimated the required activation energy for the third and final dehydrogenations (Figure 6). We

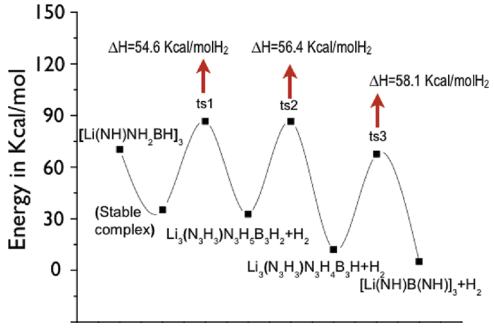

Figure 6. Third dehydrogenation from the $[Li(NH)NH_2BH]_3$ cluster.

find from Figure 6 that the system first releases some amount of energy (≈36 kcal) after the second dehydrogenation, thereby forming as a stable cluster (e.g., $[Li(NH)NH_2BH]_3$). The three consecutive hydrogen releases take place with an estimated activation barrier of 54.5, 56.4, and 58.1 kcal/mol, respectively. The reactions for third dehydrogenation are given below

$$[Li(NH)NH_2BH]_3 \rightarrow Li_3(N_3H_2)N_3H_6B_3H_2(H{-}H) \rightarrow Li_3(N_3H_2)N_3H_6B_3H_2 + H_2 \quad (9)$$

dx.doi.org/10.1021/jp210315u | J. Phys. Chem. C 2012, 116, 8859–8864

$$Li_3(N_3H)N_3H_6B_3H \rightarrow Li_3(N_3H)N_3H_6B_3H(H{-}H) \rightarrow Li_3(N_3H)N_3H_6B_3H + H_2 \quad (10)$$

$$Li_3(N_3H)N_3H_6B_3H \rightarrow Li_3(N_3)N_3H_6B_3(H{-}H) \rightarrow [Li(NH)B(NH)]_3 + H_2 \quad (11)$$

From the $[Li(NH)NH_2BH]_3$ cluster, the estimated average reaction barriers for the third dehydrogenation is still high in order to realize the process to occur at an ambient temperature. However, compared to our monomer results (85 kcal/mol) for the third dehydrogenation, using our present cluster formation mechanism, the reaction barrier is significantly decreased for cluster size $n = 3$. Thus, it is quite likely that, with the increase of cluster size (n), this reaction barrier will be further decreased to a more realistic limit. Moreover, we also predict the final product of this reaction is a cluster like complex $[Li(NH)BNH]_n$. This is in good agreement with the FTIR results found by Xia et al.[6] They found experimentally after doing elemental analysis of the dehydrogenated product of LiAB under ammonia that the final product has the chemical composition $LiNH_xBNH_{2-x}$.[6] Thus, setting $x = 1$ and 2, we have two possible options of the final product as LiNHBNH or $LiNH_2BN$. We have found that, energetically, the LiNHBNH monomer is more stable than the $LiNH_2BN$ monomer. Following our theoretical model calculation, it is quite likely that the final product will be a stable cluster of $[LiNHBNH]_n$.

H_2 Removal Energy. H_2 removal energy (E_H)[21] for monoammoniated LiAB $[Li(NH_3)NH_2BH_3]$ is defined as

$$E_H = E_{total}[Li(NH_3)NH_2BH_3] - E_{total}[Li(NH_2)NH_2BH_2] - E_{total}[H_2] \quad (12)$$

We have compared (E_H) for both monomer calculations and the cluster approach. From our monomer calculations, the estimated (E_H) values for the first, second, and third dehydrogenations for the $[Li(NH_3)NH_2BH_3]$ system are, respectively, 0.16, 0.27, and 1.3 eV/H_2. This clearly suggests that the third hydrogen is chemisorbed into the system and cannot be taken out easily. However, according to our cluster formation approach, the average values of (E_H) for the second and third dehydrogenations from the $[Li(NH_2)NH_2BH_2]_3$ cluster are, respectively, 0.25 and 0.67 eV/H_2. Therefore, it is quite clear that formation of the $[Li(NH_2)NH_2BH_2]_n$ cluster not only decrease the reaction barrier but also eases the hydrogen release from the composite system.

4. CONCLUSION

We have synthesized monoammoniated LiAB by an alternative route and noticed ≈9−11 wt % hydrogen release at 40−55 °C. The experimental observation is then combined with first-principles DFT-based model calculations to explore the underlying hydrogen release mechanism. Doing a very accurate calculation to understand the reaction mechanism of these kinds of large clusters is computationally very costly. Therefore, first, we have done some benchmark higher-level calculations (e.g., G3) and compared them with our B3LYP/MP2 results in order to understand the error bar involved in our approach. The benchmark results are comparable, and so we believe that the error bar in our calculated numbers does not affect the conclusions arrived in this paper. Theoretical results predict that the reaction is a three-step process; each step consists of 3.7, 3.9, and 4.0 wt % H_2 uptake with an altogether capacity of ≈12 wt % dehydrogenation. Although the first dehydrogenation is a direct interaction between lithium amidoborane and NH_3 monomers, the subsequent reaction steps indicate the possibility of forming higher-order nanoclusters $[Li(NH_2)NH_2BH_3]_n$. Computationally, doing a very accurate calculation (up to MP2 or MP4 level)] of a sufficiently large cluster is extremely costly, and that is why we are unable to predict the cluster size (n). However, following our model calculation, we have been able to show the relative trends for the much reduced activation barrier as well as E_H values for the $[Li(NH_2)NH_2BH_2]_3$ cluster. Our calculation predicts $[Li(NH)NHB]_n$ as the final product, which is in good agreement with the FTIR results, as found in earlier experiments.

■ ASSOCIATED CONTENT

Supporting Information

Table containing bond length comparison of monoammoniated LiAB using G3 and B3LYP/6-311++(d,p). This material is available free of charge via the Internet at http://pubs.acs.org.

■ AUTHOR INFORMATION

Corresponding Author

*E-mail: msgpd@iacs.res.in.

Present Address

[#]Fritz-Haber-Institut der Max-Planck-Gesellscaft, Faradayweg 4-6, 14195 Berlin-Dahlem, Germany.

Notes

The authors declare no competing financial interest.

■ ACKNOWLEDGMENTS

S.B. would like to thank the Physics Department of NUS for supporting his stay in NUS to carry out the research and allowing him to use the computing facility of IHPC, Singapore.

■ REFERENCES

(1) Stephens, F. H.; Pons, V.; Tom Baker, R. *Dalton Trans.* **2007**, 2613−2626.
(2) Marder, T. B. *Angew. Chem., Int. Ed.* **2007**, *46*, 8116−8118.
(3) Xiong, Z.; Yong, C. K.; Wu, G.; Chen, P.; Shaw, W.; Karkamkar, A.; Autrey, T.; Jones, M. O.; Johnson, S. R.; Edwards, P. P.; David, W. I. F. *Nat. Mater.* **2008**, *7*, 138−141.
(4) www.hydrogen.energy.gov.
(5) Wu, H.; Zhou, W.; Yildirim, T. *J. Am. Chem. Soc.* **2008**, *130*, 14834−14839.
(6) Xia, G.; Yu, X.; Guo, Y.; Wu, Z.; Yang, C.; Liu, H.; Dou, S. *Chem.—Eur. J.* **2010**, *16*, 3763−3769.
(7) Li, L.; Peng, B.; Tao, Z.; Cheng, F.; Chen, J. *Adv. Funct. Mater.* **2010**, *20*, 1894−1902.
(8) Frisch, M. J.; et al. *Gaussian 03*, revision C.02; Gaussian, Inc.: Wallingford, CT, 2004.
(9) Lee, C.; Yang, W.; Parr, R. G. *Phys. Rev. B* **1988**, *37*, 785−789.
(10) Becke, A. D. *J. Chem. Phys.* **1993**, *98*, 5648−5652.
(11) Becke, A. D. *J. Chem. Phys.* **1992**, *97*, 9173−9177.
(12) Li, L.; Peng, B.; Ji, W.; Chen, J. *J. Phys. Chem. C* **2009**, *113*, 3007−3013.
(13) Pople, J. A.; Seeger, R.; Krishnan, R. *Int. J. Quantum Chem., Symp.* **1977**, *11*, 149.
(14) Wong, B. M.; Lacina, D.; Nielsen, I. M.; Graetz, J.; Allendorf, M. D. *J. Phys. Chem. C* **2011**, *115*, 7778−7786.

(15) Gonzalez, C.; Schlegel, H. B. *J. Chem. Phys.* **1989**, *90*, 2154−2161.
(16) Collins, S. C.; Cameron, F. K. *J. Phys. Chem.* **1928**, *32*, 1705.
(17) Sullivan, E. A.; Johnson, S. *J. Phys. Chem.* **1959**, *63*, 233−238.
(18) Lee, T. B.; Mckee, M. L. *Inorg. Chem.* **2009**, *48*, 7564−7575.
(19) Shevlin, S. A.; Kerkeni, B.; Guo, Z. X. *Phys. Chem. Chem. Phys.* **2011**, *13*, 7649−7659.
(20) Kim, D. Y.; Singh, N. J.; Lee, H. M.; Kim, K. S. *Chem.—Eur. J.* **2009**, *15*, 5598−5604.
(21) Bhattacharya, S.; Wu, G.; Chen, P.; Feng, Y. P.; Das, G. P. *J. Phys. Chem. B* **2008**, *112*, 11381−11384.